Water Research 217 (2022) 118419

Contents lists available at ScienceDirect

Water Research

journal homepage: www.elsevier.com/locate/watres

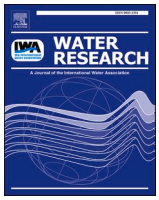

Dam construction attenuates trace metal contamination in water through increased sedimentation in the Three Gorges Reservoir

Haijian Bing [a,*], Ye Liu [a,c], Jiacong Huang [b], Xin Tian [a,c], He Zhu [a], Yanhong Wu [a]

[a] Key Laboratory of Mountain Surface Processes and Ecological Regulation, Institute of Mountain Hazards and Environment, Chinese Academy of Sciences, Chengdu 610041, China
[b] Key Laboratory of Watershed Geographic Sciences, Nanjing Institute of Geography and Limnology, Chinese Academy of Sciences, 73 East Beijing Road, Nanjing 210008, China
[c] University of Chinese Academy of Sciences, Beijing 100049, China

ARTICLE INFO

Key Words:
Trace metal contamination
Spatiotemporal variation
Sedimentary dynamics
Surface water
Fluvial sediments
Large reservoir

ABSTRACT

Dam construction has a far-reaching impact on trace metal accumulation and the metal-induced quality of the aquatic environment. However, the long-term impacts of dam construction and impoundments on the spatial distribution of trace metals and water quality remain poorly understood. Here, we found that the concentrations of trace metals in the mainstream water of the world's largest reservoir, Three Gorges Reservoir (TGR), decreased after impoundment, while their concentrations and contamination in the sediments of the water-level fluctuation zone increased significantly, especially for anthropogenic sources of metals such as cadmium, lead, and zinc. The spatial and temporal variations of anthropogenic metals in the sediments revealed increased anthropogenic dominance in their distribution under current hydrological management, especially for the urban area of the upper TGR. Sediment fluxes, particle composition, and extreme climate modulated the distribution of trace metals in the sediments. The results demonstrate that human activities have increasingly determined the distribution and contamination state of trace metals in the mainstream TGR. However, in contrast to our previously thought, the anthropogenic discharge of trace metals did not adversely affect water quality. Our results indicate that dam construction in riverine systems attenuates trace metal contamination in water through sediment sorting and deposition.

1. Introduction

Dam construction can evidently modulate the accumulation, distribution, and transportation of trace metals in riverine systems by altering factors such as the flow velocity, sediment discharge, deposition, retention, and sorting (Nilsson et al., 2005; Grill et al., 2015; Wang et al., 2016; Maavara et al., 2020). This can potentially affect water quality and human health in the catchment (Yang et al., 2012; Huang et al., 2021). According to the International Commission on Large Dams (ICOLD), more than 58,000 large dams had been built on the world's major rivers by 2020, and 40.6% of dams in China is large dam. The Yangtze River is one of Asia's largest rivers. A large number of dams have been built in the upper Yangtze River in the last few decades, and more dams are under construction or being planned (Yang et al., 2011; Xu et al., 2013; Tian et al., 2021). The Three Gorges Dam (TGD) in the upper Yangtze River is the world's largest hydroelectric dam, and the construction of the TGD has posed a profound impact on material transfer and the aquatic environment in the Three Gorges Reservoir (TGR), as well as downstream in the Yangtze River (Feng et al., 2014; He et al., 2020; Xiang et al., 2021).

One of the main characteristics of the TGR is the anti-seasonal water-level operation, which features the lowest water level (145 m) in the summer and wet seasons and the highest (175 m) in the winter and dry seasons. This results in a marked difference in the discharge of water and sediment into the reservoir relative to other flow-managed and free-flowing rivers (Tang et al., 2018a; Grill et al., 2019). Moreover, the anti-seasonal water-level operation forms a unique geomorphological unit of the water-level fluctuation (WLF) zone, which is characterized by a vertical height of 30 m and a total area of 349 km^2, and is one of the main zones for sediment accumulation in the TGR (Bao et al., 2015). Specifically, the impoundment stage in the winter and dry seasons can facilitate clear dispersal and deposition of sediments in the WLF zone,

* Corresponding author.
E-mail address: hjbing@imde.ac.cn (H. Bing).

https://doi.org/10.1016/j.watres.2022.118419
Received 18 November 2021; Received in revised form 29 March 2022; Accepted 30 March 2022
Available online 6 April 2022
0043-1354/© 2022 Elsevier Ltd. All rights reserved.

relative to the recession stage in the summer and wet seasons, which features a relatively higher duration, frequency, and magnitude of flooding. Although water recession may scour the riverbed and carry away a certain amount of sediment that was originally deposited at the impoundment stage, the WLF zone tends to maintain a stable and relatively high sediment trapping rate (Tang et al., 2016, 2018b). In addition to the variable sediment loads, the special flow regime under dam operation also affects sediment sorting and thus modulates sediment redistribution in the WLF zone. For example, the preferential settling of coaster particles has been observed in backwater sections that have a relatively low flow velocity (Bing et al., 2019a; Tang et al., 2018b).

Sediments are the predominant sinks of trace metals in rivers, and their dynamics and fluxes determine the biological availability, distribution, and environmental accessibility of trace metals in aquatic environment to a large extent (Du Laing et al., 2009; Baborowski et al., 2012; Zhang et al., 2014). Under annual cyclic exposure and inundation, the WLF zone in the TGR mainstream faces many strong anthropogenic and natural disturbances, such as secondary geological disasters, soil erosion, and tillage (Bao et al., 2015; Xu et al., 2013), which may cause the migration of accumulated sediments from the WLF zone and increase the release of trace metals to the overlying water. Moreover, sediment fluxes in the WLF zone are appreciably influenced by sediment management strategies in the TGR, such as the cascade reservoirs that were constructed in the upper Yangtze River, sediment regulation policies, and soil and water conservation projects in the catchment (Yang et al., 2018; Ren et al., 2020; Ren 2021). Relative to the pre-dam period, the sediment input into the TGR decreased sharply from 2003 to 2012 and decreased further to approximately zero from 2013 to 2017 (Yang et al., 2011, 2014; Dai et al., 2014; Tian et al., 2021). This potentially determines the distribution and ecological risk of trace metals in the sediments (Gao et al., 2019; Bing et al., 2019a). In addition, the ecological, environmental, and geomorphological conditions in the WLF zone of the TGR mainstream over the post-dam period are still highly dynamic under the special flow regime and increasing anthropogenic disturbance (Bao et al., 2015), which directly affects sediment dynamics and the metals associated with them. A recent modeling study predicted that it would take 320−560 years to reach the sedimentation balance in the TGR under current water-sediment conditions (Chen et al., 2021). Therefore, a long-term and continuous focus on trace metal contamination in sediments is necessary to control the water quality in the TGR.

Anthropogenic disturbances along rivers are distinctly position-dependent, yet current frameworks or models of environmental impact assessment generally render all river reaches equally important irrespective of habitat suitability or local human influence (Xenopoulos and Lodge, 2006; Grill et al., 2015), which may cause uncertainty in the prediction of dam-induced environmental impacts. Spatiotemporal information on trace metal contamination in riverine systems provides a proxy for anthropogenic disturbance. Because of its non-degradation and toxicity to aquatic organisms and human health, the contamination of trace metals in the aquatic environment of the TGR has been a concern since the construction of the TGD (Yang et al., 2012). Many previous studies have found that after the full operation of the TGR, trace metals such as Cd, Cr, Cu, Pb, and Zn in the water did not exceed the quality standards of drinking water and/or surface water in China, whereas the contamination of some metals such as Cd, Pb, and Zn in the sediments reached a moderate or even high level (Bing et al., 2016; Gao et al., 2016; Lin et al., 2020). Meanwhile, the spatial distribution of trace metals in the sediments has changed markedly with periodic flow management; moreover, the changes in geomorphological characteristics, local human activities, and sediment fluxes in the WLF zone have been regarded as the main drivers of spatial variations in trace metal distribution (Bing et al., 2019a; Gao et al., 2019; Lin et al., 2020). However, the majority of these studies mainly consider either a short time scale (i.e., one or two impoundment periods), or the relatively small spatial scale as the study unit, thereby overlooking the long-term and large-scale spatial variations in the contamination of trace metals in the water and/or sediments at all phases of the dam's life. As such, the direction and magnitude of trace metal contamination in space and time, as well as the underlying drivers, are still unclear and deserve to be comprehensively explored. In addition, extreme climate and flooding in the upper basin of the Yangtze River have become increasingly anomalous and more frequent in recent years (Li et al., 2021; Zhou et al., 2021). This is believed to not only affect the river runoff and sediment transfer, but also regulate the distribution and contamination of trace metals in the WLF zone of the TGR. Overall, in terms of the global surge in dam construction (Grill et al., 2015; Zarfl et al., 2015), it is of paramount importance to consider the spatial and temporal variations of trace metal contamination in the water and sediments of dammed rivers over the long term in order to improve aquatic quality; this would also provide insights into the dynamics of trace metals in the water-sediment system under long-term and periodic flow management, as well as extreme climate change.

In combination with other short-term or single monitoring of trace metals in the water and/or sediments of the TGR mainstream, this study explored the impact of long-term hydrological management with TGD construction on the dynamics of trace metals in the sediments and overlying water. To achieve this, the WLF zone in the entire mainstream of the TGR was selected to measure six trace metals including Cd, Cr, Cu, Ni, Pb, and Zn in the water and sediments during 2014–2020. The main objectives were to: 1) plumb the spatial and temporal variations in the distribution and contamination of trace metals in the water and sediments, 2) identify the anthropogenic effects on the accumulation of trace metals by the spatiotemporal distribution and Pb isotopic ratios, and 3) decipher the effects of sedimentary dynamics on the variations in trace metals and aquatic environment quality. We expected that local anthropogenic sources of trace metals would become increasingly dominant in the aquatic environment because of decreasing sediment inputs from the upper Yangtze River. As a result, the increased trace metals might negatively affect the quality of the overlying water; however, the particle composition could play a vital role in regulating the contamination of trace metals in the TGR.

2. Materials and methods

2.1. Study area

The region of the TGR (28°28′−31°44′N, 105°49′−110°12′E) covers the upper Yangtze River between Chongqing and Yichang, with a total water surface area of 1080 km^2 and a storage capacity of 39.3 billion m^3 at a water level of 175 m (Fu et al., 2010). The study area spanned the entire mainstream of the TGR, with a length of more than 660 km (Figure S1). The climate in the TGR region is mainly controlled by a humid subtropical monsoon with the mean annual temperature and mean annual precipitation of 16–19 °C and 1000–1200 mm, respectively. There were three major types of bedrock in the study area: purple and red rocks (74%), carbonate (19%) and other rocks (7%) (Bao et al., 2015; Tang et al., 2016).

2.2. Sample collection and preparation

In the summer season, at the time of the lowest water level (145 m) in 2014, 2016, 2018 and 2020, the same sites (except one site, Banan, in 2014) in the WLF zone below 150 m were campaigned to collect surface sediments (0–20 cm). A two-year sampling interval allowed us to obtain the newly deposited sediments because of the high sedimentation rate and flow regulation in the TGR (Tang et al., 2016; Zhu et al., 2019). At each site, at least three 10 × 5 m plots were randomly selected with the distance between each greater than 20 m, and at each plot, five samples were collected with a plastic shovel and mixed into one sample on site. To remove the sediments below 20 cm, we first collected sediment blocks with 10 × 5 × > 20 cm and then excluded the sediments below 20 cm. In total, 312 sediment samples, comprising 81, 63, 78, and 90 in

2014, 2016, 2018, and 2020, respectively, were collected in the WLF zone. In 2016, 2018, and 2020, one background site (Zhutuo) outside the TGR was selected to sample additional sediments ($n = 3$ per year) according to the same method. All samples were stored at 4 °C in the field, and after returning to the laboratory, the samples were freeze-dried and sieved to < 2 mm to remove coarse particles and plant residues. One portion of the sample was used to analyze the sediment properties, and the other was pulverized using an agate mortar to pass through a 100-mesh nylon screen for the analysis of element concentrations and trace metal fractions.

Surface water samples were collected in the TGR mainstream when collecting the sediment samples in 2016 ($n = 18$) and 2020 ($n = 29$). Three repeated samples (0–50 cm) were collected at each site using a depth-keeping water sampler made of polymethyl methacrylate, and then mixed into one sample on site. The samples were acidified with HNO_3 solution (volume ratio of water: HNO_3 = 100:1) and stored in polyethylene bottles at 4 °C according to the Technical Regulation of the Preservation and Handling of Samples of China (HJ 493–2009). Once in the laboratory, the water samples were passed through a 0.45 μm filter membrane for further analysis of the dissolved metal concentrations.

2.3. Chemical analysis

Sediment grain sizes (clay, < 4 μm; silt, 4–64 μm; sand, > 64 μm) were measured using a Mastersizer 2000 Laser Grain-size Meter after the removal of carbonates and organic matter using HCl and H_2O_2, respectively. A grain size of less than 64 μm was defined as fine particles. The pH was analyzed using a pH meter after mixing the sediments and deionized water at a ratio of 1:2.5 for 30 min. The organic matter content was determined using the loss on ignition (LOI) test. A known amount of sample was burned at 550 °C for 4 h in a muffle furnace, and the percentage of weight loss was recorded.

The fractions of trace metals (Cd, Cr, Cu, Ni, Pb, and Zn) in the sediments were analyzed following the European Standard, Measurements, and Testing program, formerly the Community Bureau of Reference (BCR) method, which includes acid-soluble (or exchangeable and carbonate-bound fraction), reducible, oxidizable, and residual fractions (Rauret et al., 1999). The acid-soluble fraction of trace metals, defined as the labile fraction, was analyzed in this study to reveal the metals' mobility and ecological risk in sediments. The sediment samples used for the analysis of total metal concentrations were digested with a mixture of concentrated acids, comprising HF, HNO_3, $HClO_4$, and HCl (Bing et al., 2014). The concentrations of the major elements (Al, Ca, Fe, Mg, Mn, and Ti) in the digestion solution were measured using an inductively coupled plasma atomic emission spectrometry, and the concentrations of trace metals were determined using inductively coupled plasma mass spectrometry (ICP-MS). Quality control was ensured by the analysis of blanks, duplicate samples, and reference materials (GSD-9 and GSD-11). The precision and accuracy were routinely below 5% according to the relative standard deviation (RSD) of the repeated samples and standard reference materials. The concentrations of the trace metals in the filtered water were measured using ICP-MS. The calibration blank and independent verification standard were analyzed every five samples to calibrate the precision of the instrument. The concentration of the blanks was < 1% for all metals, and the analysis precision of the triplicate samples was < 5% for the RSD.

The Pb isotopic ratios of $^{208}Pb/^{206}Pb$ and $^{206}Pb/^{207}Pb$ in the sediments were determined using ICP-MS (Agilent 7700 ×) to identify the anthropogenic contribution to Pb and the metals that had similar sources as Pb. Standard reference materials from the United States National Institute of Standards and Technology SRM 981 ($^{208}Pb/^{206}Pb = 2.1681 \pm 0.0008$; $^{207}Pb/^{206}Pb = 0.9146 \pm 0.0003$) were used for instrument calibration and quality control. With multiple measurements of the standard SRM 981, $^{208}Pb/^{206}Pb$ (2.135 ± 0.0016) and $^{207}Pb/^{206}Pb$ (0.869 ± 0.0009) were analyzed with a precision (RSD) of < 0.07% and < 0.12%, respectively.

2.4. Contamination indices

The geoaccumulation index (I_{geo}) was used to assess the contamination levels of trace metals in the sediments (Muller, 1969).

$$I_{geo} = log_2(C_i / 1.5C_0) \quad (1)$$

where C_i is the concentration of a metal, C_0 is its background in the soils of Chongqing Municipality (Cd, Cr, Cu, Ni, Pb, and Zn: 0.084, 50.5, 19.1, 23.9, 21.4, and 51.7 mg/kg, respectively) (Chen et al., 2015), and the coefficient 1.5 is used to detect natural background influence (Loska et al., 2004). Seven classes were divided according to I_{geo}: uncontaminated ($I_{geo} \leq 0$), uncontaminated to moderately contaminated ($0 < I_{geo} \leq 1$), moderately contaminated ($1 < I_{geo} \leq 2$), moderately to heavily contaminated ($2 < I_{geo} \leq 3$), heavily contaminated ($3 < I_{geo} \leq 4$), heavily to extremely contaminated ($4 < I_{geo} \leq 5$), or extremely contaminated ($I_{geo} > 5$).

The integrated pollution load index (*PLI*) was used to assess the overall contamination state of the sediments by all the metals (Luo et al., 2012).

$$PLI = (PI_1 \times PI_2 \times PI_3 \times \ldots \times PI_n)^{1/n} \quad (2)$$

where $PI = C_i/C_0$ and n is the metal number. Contamination was classified as: background ($PLI = 0$), uncontaminated ($0 < PLI \leq 1$), uncontaminated to moderately contaminated ($1 < PLI \leq 2$), moderately contaminated ($2 < PLI \leq 3$), moderately to highly contaminated ($3 < PLI \leq 4$), highly contaminated ($4 < PLI \leq 5$), or very highly contaminated ($PLI > 5$).

2.5. Statistical analysis

One-way analysis of variance (ANOVA) was applied to examine the differences in the concentrations and contamination levels of trace metals in the sediments and water, while the Spearman correlation analysis (two-tailed) and regression analysis were applied to establish the relationships between the studied variables. Fisher's test was used to examine significant differences at $p < 0.05$. Finally, linear and nonlinear regression were used to display the spatial distribution patterns of sediment properties and the concentrations and contamination indices of trace metals in the water and sediments. All statistical analyses were performed using the SPSS 19.0 and Origin 8.0 for Windows.

3. Results

3.1. Basic characteristics of sediments

The basic properties of the sediments, including grain size, organic matter, pH, and major elements during 2014–2020 are presented in Table S1. Relative to other properties in the sediments, we observed marked spatiotemporal variations in the contents of grain size, Al, and Fe. Specifically, fine particles, including clay and silt, dominated the grain sizes of the sediments, and their contents increased from 2014 to 2018, but then decreased in 2020 to the levels of 2014 and 2016 (Fig. 1a). Similarly, the concentrations of Al and Fe in the sediments also increased evidently from 2014 to 2018, and then decreased in 2020 (Fig. 1b, c). Spatially, the contents of fine particles, Al, and Fe showed an evident increase towards the dam, and their contents increased markedly from 2014 to 2018 with increasing distance towards the dam, although they decreased again in 2020 (Fig. 1d, e, f).

3.2. Spatiotemporal distribution of trace metals in the sediments and surface water

Compared with the early stage of the impoundment in 2010, the concentrations of trace metals (especially Cd, Pb, and Zn) in the sediments increased markedly since the full operation of the TGR (since

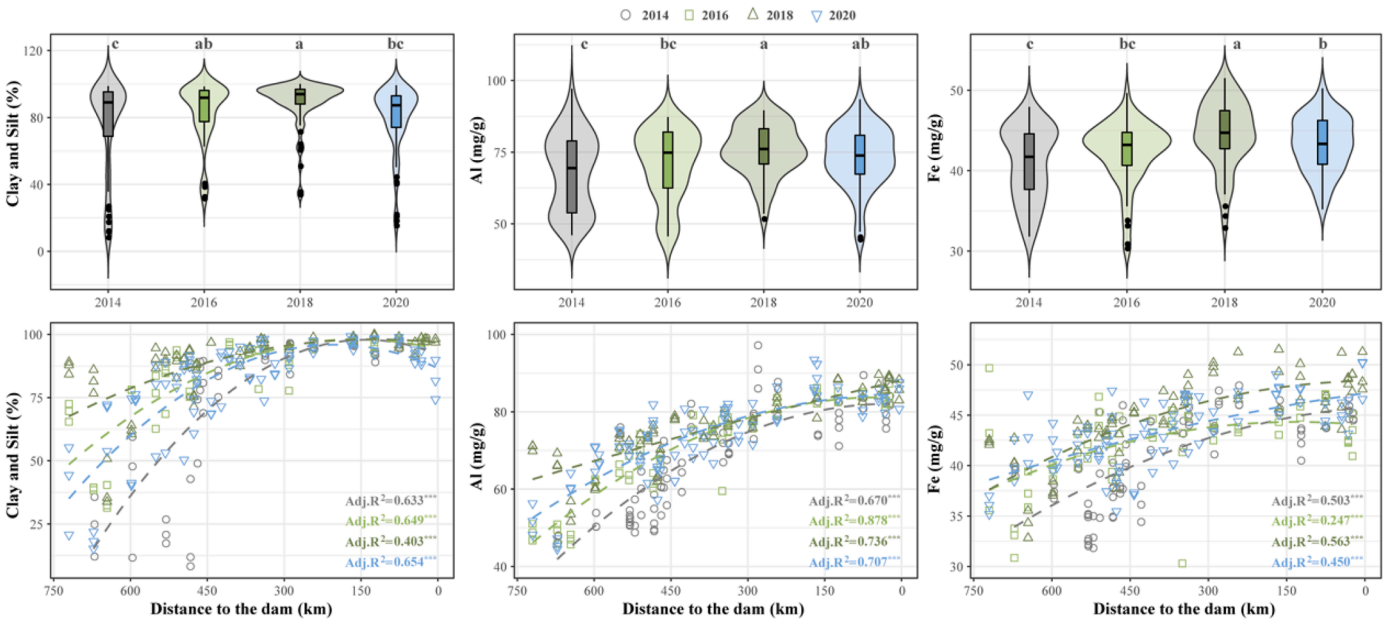

Fig. 1. Temporal and spatial characteristics of fine particles (clay and silt), Al, and Fe in the sediments during 2014–2020. The different letters in the sub-figures (a), (b), and (c) represent a significant difference of the values among the four years ($p < 0.05$). The fitting curves in the sub-figures (d), (e), and (f) show the significant spatial variation trend of each variable towards the dam. ***, $p < 0.001$.

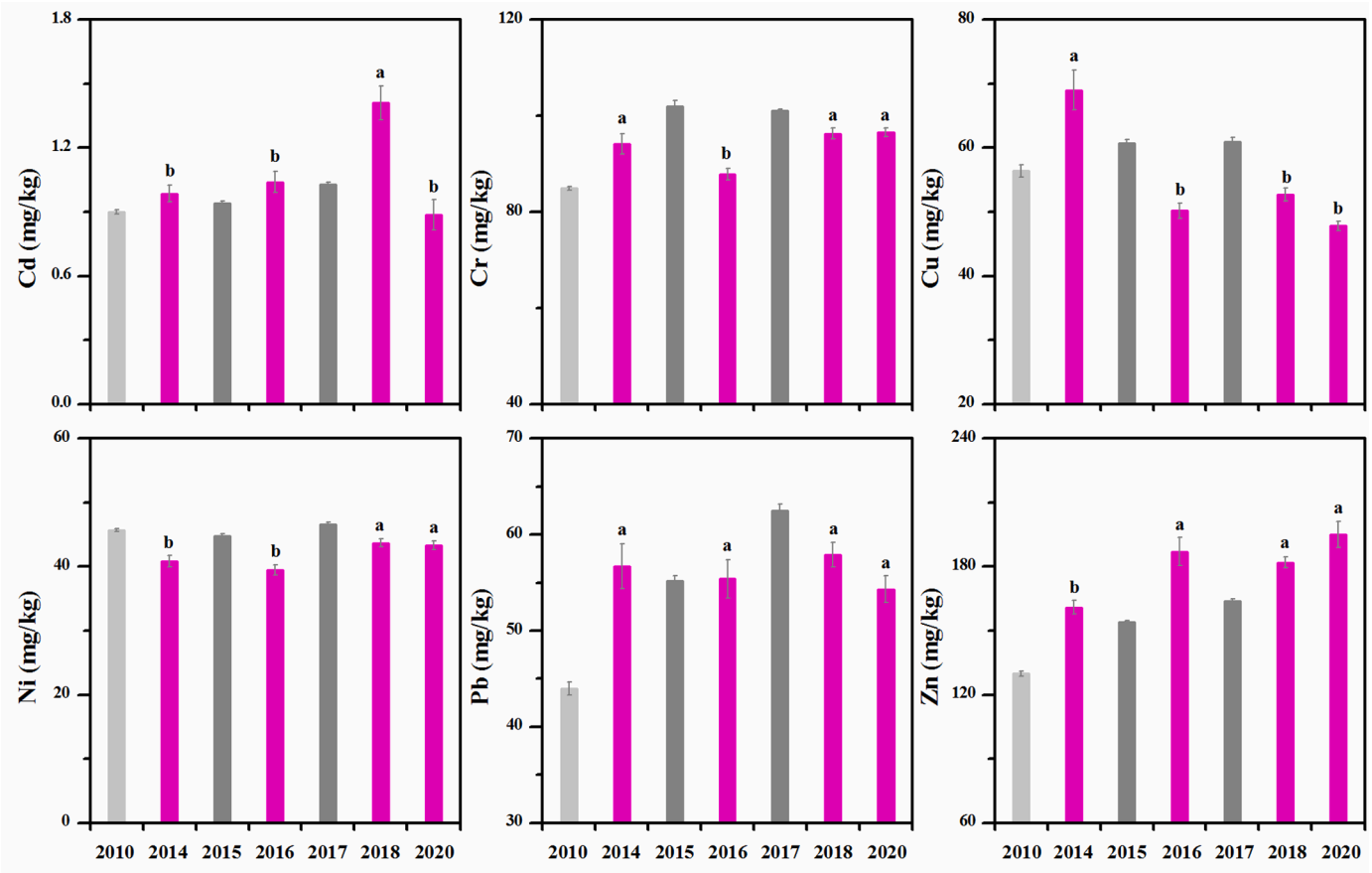

Fig. 2. Concentrations of trace metals (mean ± SE) in the sediments of the TGR. The data at the early stage of the impoundment operation in 2010 (light gray, $n = 73$) were cited from Gao et al. (2015) and the data after the full impoundment operation in 2015 and 2017 (dark gray, $n = 47$) were cited from Gao et al. (2019). Only the data in this study (magenta) were compared using ANOVA, and the different letters represent a significant difference of the metal concentrations among the four years ($p < 0.05$).

2012), although a slight fluctuation in the concentrations existed for specific metals (Fig. 2). Among the four years in this study, significantly higher concentrations were observed for Cd in 2018, Cu in 2014, and Ni in 2018 and 2020, while lower values were observed for Cr in 2016 and Zn in 2014. No significant changes in Pb concentrations were observed over the four years. In contrast, there was marked spatial variation in the metal concentrations in the sediments during 2014–2020 (Fig. 3). In 2014, the concentrations of all trace metals (except Cu) showed an increasing trend towards the dam. However, although the concentrations of Cr (except in 2016) and Ni continued to increase towards the dam following 2016, other trace metals changed their spatial distribution patterns. In 2016 and 2020, the concentrations of Cd, Cu, Pb, and Zn showed an increasing trend in the upper section of the TGR (approximately 550 km away from the dam) and then decreased appreciably despite a slight increase in the WLF zone near the dam. In 2018, Cu did not show a marked variation along the TGR, while a significant decrease in the concentrations of Cd, Pb, and Zn towards the dam was observed.

Owing to the low mobility of Cr and Ni in the sediments, the concentrations and percentages of labile Cr (< 1.0 mg/kg and $< 1\%$ of total Cr) and Ni (< 2.0 mg/kg and $< 5\%$ of total Ni) were very low according to the BCR method. Thus, we only displayed the spatiotemporal variations in the concentrations and percentages of labile Cd, Cu, Pb, and Zn. The labile Cd concentrations showed an increasing trend from 2014 to 2018 and then decreased in 2020. The percentage of labile Cd to total Cd exceeded 50%, and was significantly higher in 2016 and 2018, followed by 2020 and then 2014 (Fig. 4A). The labile Cu concentrations decreased from 2014 to 2020, and the percentage showed a similar trend as its concentrations, varying between 10% and 15% in 2014, and between 5% and 10% in other years. The labile Pb concentrations were significantly higher in 2014 and 2018, followed by 2016 and then 2020, and its percentage was higher in 2014 ($> 5\%$) than in other years ($< 5\%$). The labile Zn concentrations were significantly higher in 2016, 2018, and 2020 than in 2014, while its percentage was higher in 2016 and 2018 (15–20%) than in 2014 and 2020 (10–15%). Spatially, the distribution of labile metals was similar to that of the total metals (Fig. 4B), except for Cu, Pb, and Zn in 2014, which were relatively higher in the upper section of the TGR.

The concentrations of trace metals in the surface water were very low in 2016 and 2020, far below the standards of drinking water quality and surface water quality (I type) in China (Table 1). Meanwhile, the concentrations of trace metals decreased notably from 2008 to 2020, except for Zn, which exhibited marked annual fluctuations. Spatially, the concentrations of trace metals in the water were generally consistent with their concentrations in the sediments (Figure S2). The concentrations of Cd, Cu, Pb, and Zn were relatively higher in the upper section of the TGR (except Pb in 2020), while an increasing trend of Cr and Ni towards the dam was observed despite the marked decrease in their concentrations in 2020. Similar spatial distribution patterns of trace metals existed in the water and sediments, whereas a significant correlation of the concentrations between the water and the sediments was not observed, except for Zn (Adj.$R^2 = 0.110$, $p = 0.013$). In contrast, the concentrations of Cd, Cu, Pb, and Zn in water were significantly correlated with their labile fractions in the sediments (Figure S3).

3.3. Contamination state of trace metals in the sediments

According to the I_{geo}, Cd contamination was significantly higher (moderate to high level) than other metals, followed by Zn (moderate level), and Cr, Cu, Ni, and Pb with nil to moderate contamination (Table 2). Compared with other years, the contamination of trace metals was evidently higher for Cd (high level) in 2018, Cr and Ni in 2018 and 2020, Cu in 2014, and Zn in 2016, 2018, and 2020, while Pb contamination did not show a temporal difference. Moreover, the spatial distribution of I_{geo} was generally similar to that of the metal concentrations (Figure S4). The *PLI* results showed that the sediments were moderately to highly contaminated by all metals, and the contamination in 2018 was relatively higher than that in 2016 and 2020. Spatially, the contamination increased significantly towards the dam in 2014, yet the opposite case was observed in 2018; in 2016 and 2020, the contamination increased towards the dam in the upper section of the TGR and then decreased markedly (Fig. 5).

The percentage of labile metal concentration to its total concentration, known as the risk assessment code (RAC), provides an index to assess the risk of trace metals in the sediments for aquatic organisms (Singh et al., 2005). The RAC classification was defined as: $\leq 1\%$, no risk; 1–10%, low risk; 10–30%, moderate risk; 30–50%, high risk; $> 50\%$, extremely high risk. According to this classification, the risk of Cd in the sediments for aquatic organisms reached an extremely high level each year, Zn had a moderate risk, Cu (except in 2014, moderate risk), Ni, and Pb had a low risk level, and Cr had no risk (Fig. 4A).

3.4. Isotopic ratios of Pb in the sediments

Although the concentrations of Pb in the sediments did not show a significant difference during 2014–2020, its isotopic ratios were relatively low for $^{206}Pb/^{207}Pb$ in 2020 and $^{208}Pb/^{206}Pb$ in 2018 (Table S2). Meanwhile, there was a marked spatial variation in the Pb isotopic ratios among the four years. The ratio of $^{206}Pb/^{207}Pb$ did not change significantly along the mainstream in 2014 ($p = 0.114$), despite the relatively low values in the upper section, while it showed significantly different distribution patterns in the other three years ($p < 0.001$, Fig. 6A); particularly, the ratio of $^{206}Pb/^{207}Pb$ in 2016 evidently decreased from the upper section, and then increased again in the area near the dam, while the ratio in 2018 displayed a prominent increase towards the dam. Further, the ratio in 2020 decreased largely in the upper section, increased again in the middle section, and then remained stable.

According to the diagram of $^{206}Pb/^{207}Pb$ versus $^{208}Pb/^{206}Pb$ in the sediments and potential source materials, we observed three main characteristics (Fig. 6B). First, there was a significant correlation between $^{206}Pb/^{207}Pb$ and $^{208}Pb/^{206}Pb$ over the four years, and the significance increased markedly from 2014 to 2020, indicating a much clearer anthropogenic versus natural signal in the sediments. Second, the absolute slopes of the fitting lines evidently increased from 2014 to 2020, and according to the Pb isotopic ratios, more plots with much lower $^{206}Pb/^{207}Pb$ and higher $^{208}Pb/^{206}Pb$ were close to anthropogenic endmembers in 2018 and 2020 than in the other years (see the sub-figure in Fig. 6B). Third, the ratios in most of the plots overlapped with those in ores, coal emissions, and air dust or aerosols in southern China, but not in natural endmembers (e.g., background soils in southern China's mountains) or vehicle emissions. Meanwhile, the ratios of $^{206}Pb/^{207}Pb$ and $^{208}Pb/^{206}Pb$ in the sediments, especially in 2018 and 2020, were close to those in the mosses from southern China's mountains where Pb was identified from anthropogenic sources (Bing et al., 2019b). Furthermore, because the $^{206}Pb/^{207}Pb$ ratio has been widely used to identify Pb sources in the environment (Chen et al., 2005; Cheng and Hu, 2010), we also compiled the ratios from various archives in southern and southwestern China. The results further support that Pb in the sediments was mainly from anthropogenic sources, including ore mining and smelting, fossil fuel combustion, and atmospheric deposition (Table S2).

3.5. Relationship of trace metals with sediment variables

There was a clear difference in the correlation of trace metals in the sediments between sampling years (Fig. 7). Although a significant correlation was observed between trace metals (except Cr and Zn in 2014) in 2014 and 2016, the correlation coefficients between Cd, Cu, Pb, and Zn increased significantly in 2016. In 2018, Cd, Pb, and Zn were significantly and positively correlated with each other, whereas they showed a negative or non-significant correlation with Cr and Ni, which correlated significantly with each other. A positive correlation between Cu and all other metals, except Cd, was observed in 2018. In 2020, the

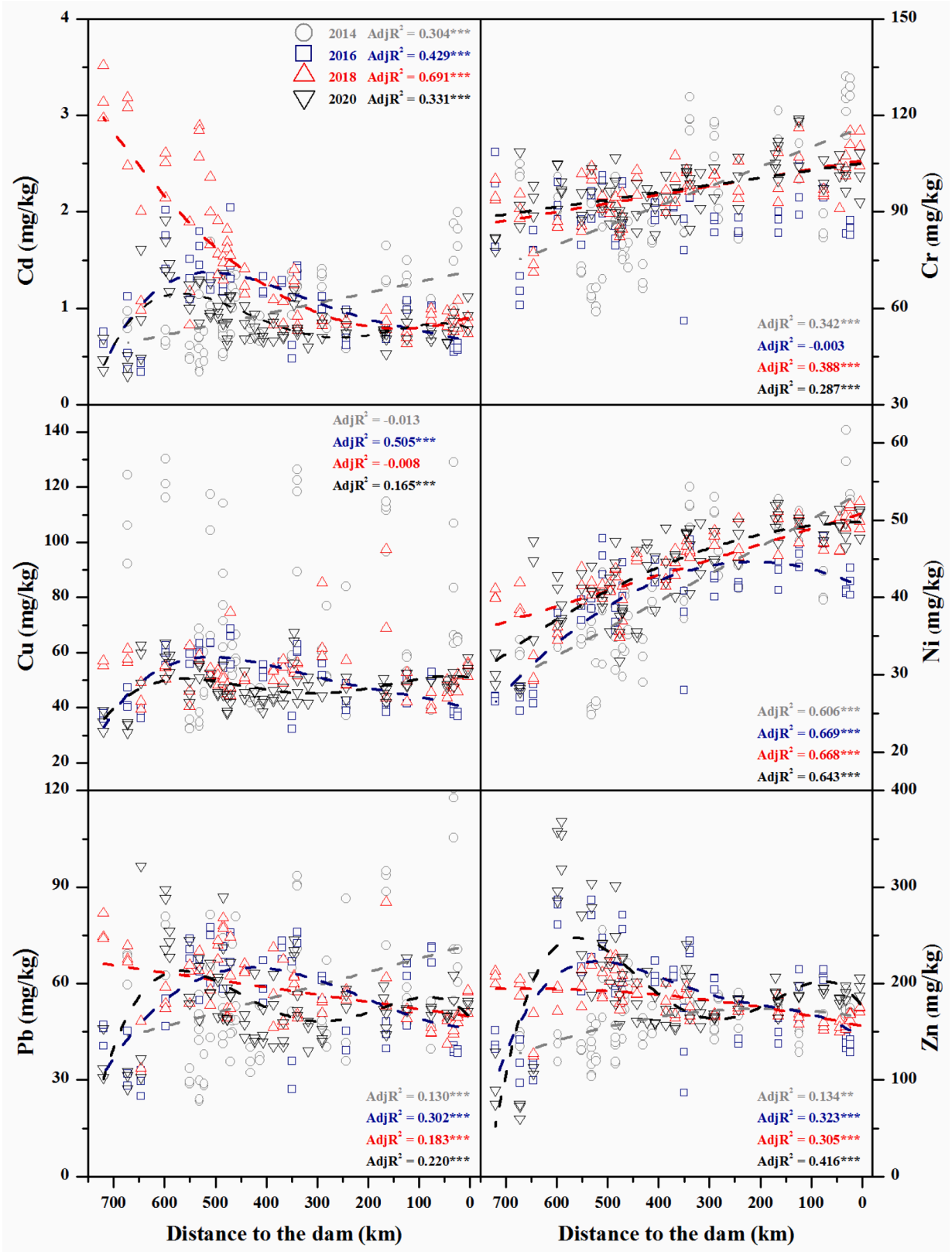

Fig. 3. Spatial and temporal distribution of trace metals in the sediments of the WLF zone. The fitting curves highlight the spatial variation trend of each metal towards the dam. **, $p < 0.01$, ***, $p < 0.001$.

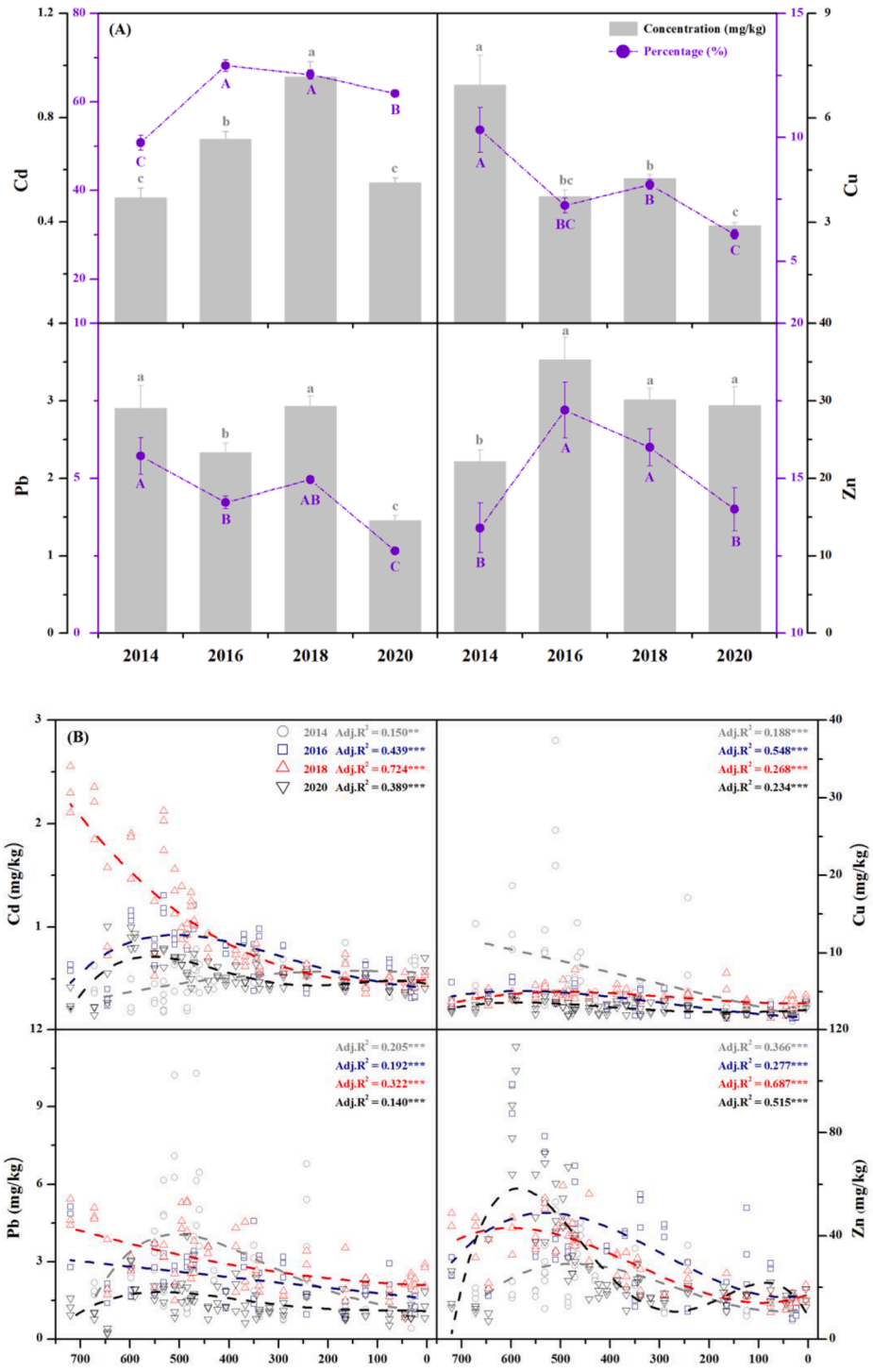

Fig. 4. Temporal and spatial characteristics of labile Cd, Cu, Pb, and Zn in the sediments of the WLF zone. The different lowercase letters in the Fig. 4A represent significant differences in the metal concentrations, and the different capital letters represent significant differences in the percentage (blue color) of the concentration of the labile fraction to its total concentration ($p < 0.05$). The fitting curves in Fig. 4B show the significant spatial variation trend of each labile metal towards the dam. **, $p < 0.01$, ***, $p < 0.001$.

correlations of Cd, Pb, and Zn were still significant, and a similar case was also observed for Cr and Ni; however, the correlations of Cd, Pb, and Zn with Cr and Ni were not significant, except for a weak correlation between Cr and Pb. Copper showed a significant positive correlation with all other metals in 2020.

The correlation between trace metals and sediment properties was metal- and year-specific (Fig. 7). Except for Cd and Zn in 2014, which were positively correlated with fine particles, Cd, Pb, and Zn showed a non-significant or negative correlation with fine particles, and they did not positively correlate with LOI and pH (except Pb in 2014) in any year. Moreover, Cd, Pb, and Zn had no or a negative correlation with other major elements (except Mn) in the sediments sampled from 2016 to 2020, whereas they showed a significant and positive correlation with Al, Fe, and Mg in 2014. In contrast, Cr and Ni correlated significantly and positively with fine particles, Al, and Fe each year (except Cr vs. Al in 2016). Copper had a weak correlation with fine particles, LOI, pH, and Al each year, and it correlated significantly with other major elements (except Fe) in 2016.

Table 1
Concentrations of trace metals (mean ± SE, μg/L) in the water of the TGR mainstream in 2016 and 2020. The data in other reports and the relevant standards of water environmental quality in China are also presented.

Sampling time	Cd	Cr	Cu	Ni	Pb	Zn	Refs
2016 (n = 18)	0.023±0.001[a]	0.869±0.014[a]	1.32±0.03[a]	2.73±0.03[a]	0.019±0.001[a]	1.11±0.03[b]	This study
2020 (n = 29)	0.026±0.001[a]	0.134±0.004[b]	0.835±0.015[b]	0.460±0.004[b]	0.017±0.001[a]	3.56±0.11[a]	
2008	1.475	–	10.369	–	15.025	–	Gao et al. (2016)
2013	0.771	–	3.013	–	7.893	10.431	Gao et al. (2016)
2015 (dry season)	0.045	0.490	1.735	–	0.526	128.0	Zhao et al. (2017)
2015 (rainy season)	0.031	0.453	1.744	–	1.637	128.5	Zhao et al. (2017)
2015–2016	0.003–0.368	0.13–5.20	0.22–18.8	–	0–8.98	1.91–103.7	Zhao et al. (2020)
2015–2016	0.02	0.47	1.21	–	0.04	12.98	Lin et al. (2020)
The standards of water quality in China							
Drinking water quality [a]	5	50	1000	20	10	1000	GB5749–2006
Surface water quality (I type) [b]	1	10	10	–	10	50	GB3838–2002

[a] Standards for drinking water quality, China (GB5749–2006).
[b] National surface water environmental quality standards (GB3838–2002).
The different lowercase letters represent significant differences in trace metal concentrations between 2016 and 2020 ($p < 0.05$). The data of the water sampled in 2008 and 2013 include the sites in upper Yangtze River and the tributary rivers of the TGR, and the specific information can be found from Gao et al. (2016).

Table 2
Contamination characteristics of trace metals in the sediments during 2014–2020.

Variables	2014 (n = 81)	2016 (n = 60)	2018 (n = 75)	2020 (n = 87)
Geoaccumulation index (I_{geo})				
Cd	2.86±0.06 b	2.93±0.08 b	3.32±0.08 a	2.74±0.05 b
Cr	0.28±0.03 b	0.21±0.02 c	0.34±0.02 ab	0.34±0.01 a
Cu	1.16±0.06 a	0.78±0.04 bc	0.86±0.02 b	0.72±0.02 c
Ni	0.16±0.03 b	0.12±0.03 b	0.27±0.02 a	0.26±0.02 a
Pb	0.73±0.06 a	0.73±0.05 a	0.82±0.03 a	0.72±0.04 a
Zn	1.03±0.03 b	1.21±0.05 a	1.22±0.02 a	1.27±0.05 a
Integrated contamination index (*PLI*)	3.16±0.08 ab	3.06±0.08 b	3.33±0.05 a	3.06±0.05 b

The different lowercase letters represent significant differences in each variable over the four years ($p < 0.05$).

4. Discussion

4.1. Increasing anthropogenic dominance on trace metal contamination during dam operation

Dam construction can dramatically slow down flow velocity and increase water retention time, causing the subsequent capture of sediments in reservoirs (Feng et al., 2014; Latrubesse et al., 2017; Tian et al., 2021; Xiang et al., 2021), which may enrich trace metals in aquatic environment because of sediment adsorption effects. As expected, we observed an evident increase in the concentrations of trace metals in the sediments of the WLF zone after the full impoundment stage since 2012 when compared with the pre-dam period (before 2002, Xu et al. (1999)) and the early stage of the post-dam period (2003–2012, Fig. 2). Meanwhile, the concentrations of trace metals in the sediments after the full impoundment exceeded their local background of > 10-fold for Cd, 3- to 4-fold for Zn, 2- to 3-fold for Cu and Pb, and nearly twice for Cr and Ni from 2014 to 2020, and the values of each metal exceeded their individual threshold effect level for aquatic organisms (MacDonald et al., 2000). As such, the sediments were moderately to highly contaminated with the trace metals and featured a high potential risk (Table 2). However, there was a marked difference in the contamination levels for specific trace metals in the sediments, which was characteristic of relatively high contamination for Cd, followed by Cu, Pb, and Zn, and then Cr and Ni (Table 2, Fig. 4A). This indicates that Cd should be of great concern in the WLF zone of the TGR over the long term in terms of its high toxicity to aquatic organisms. Meanwhile, trace metals in the sediments can likely be characterized by distinctly different anthropogenic versus natural sources.

The correlation analysis clearly identified three groups of trace metals in the sediments, along with temporal variations from 2014 to 2020 (Fig. 7). The first group, including Cd, Pb, and Zn, showed a consistent positive correlation with each other in any year, whereas they had a non-significant and even negative correlation with fine particles, Al, and Fe in 2018 and 2020 relative to 2014 and 2016, which suggests an increasing anthropogenic contribution to these metals. Although the concentrations of Pb in the sediments did not increase significantly during 2014–2020, which may be related to the large range of Pb concentrations at such a large spatial scale that affects the statistical significance, the marked increase in Pb concentrations since the full operation of the TGR (e.g., since 2014) supports the increased anthropogenic influence (Fig. 2). Moreover, the Pb isotopic ratios further confirmed the increasingly evident anthropogenic signal of Pb in the sediments, which exhibited an increase in the correlation coefficients from 2014 to 2020 and an overlap of the plots in the sediments with multiple anthropogenic endmembers in 2018 and 2020 (Fig. 6B). Meanwhile, increasing human activities in the catchment have also increased pollutant emissions under intensifying industrial production (Figure S5b-c). Recent studies have reported that trace metals such as Cd, Pb, and Zn in the sediments and/or water of the TGR are related to anthropogenic emissions from the catchment, including industrial emissions involved in coal utilization and ore smelting, agricultural emissions such as chemical fertilizers and herbicides, and shipping-related emissions (Gao et al., 2019; Zhao et al., 2020). Although our Pb isotopic ratios did not reveal the agricultural and vehicle/shipping fuel-oil sources of Pb, the ratios in the sediments overlapped with those in air dust or aerosols, indicating the complicated and mixed anthropogenic sources of Pb and metals that correlated significantly with Pb. The second group included Cr and Ni, which were significantly and positively correlated with each other from 2014 to 2020, but not with Cd, Pb, and Zn in 2018 or 2020, also had a significant correlation with the fine particles and mineral elements (e.g., Al, Fe, Ca, and Mg) despite a small difference among the years. This suggests that Cr and Ni have different sources of Cd, Pb, and Zn, and are mainly from natural origins. Copper, as the third group, generally had a close correlation with all other trace metals, indicating a mixed source from both anthropogenic and natural origins. In addition to the difference in the metal sources, the significant correlation of Fe, Mn, Ca, and Mg with specific trace

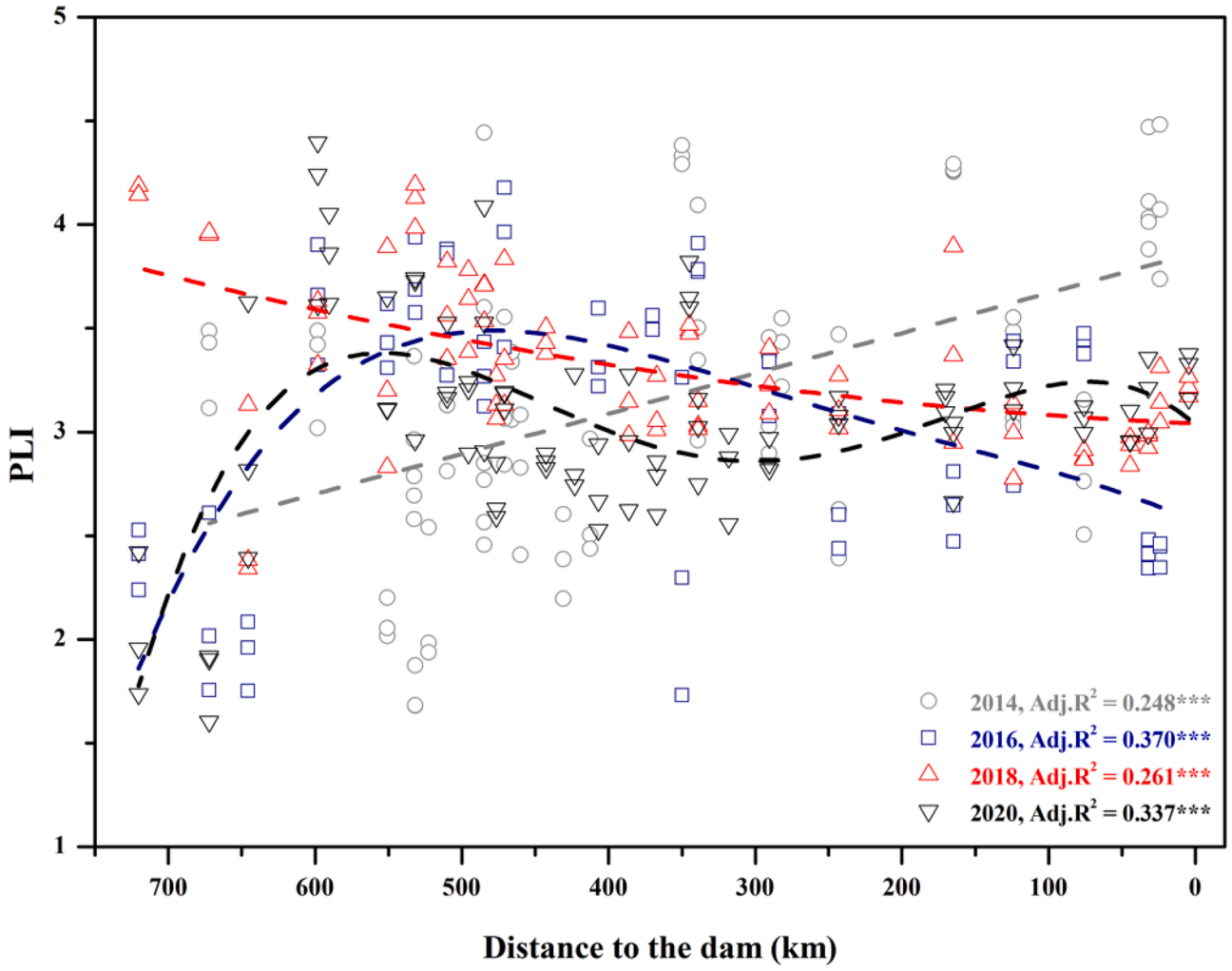

Fig. 5. Spatial and temporal variations in the integrated contamination index (*PLI*) of trace metals in the sediments of the WLF zone. The fitting curves show the significant spatial variation trend of the *PLI* towards the dam. ***, $p < 0.001$.

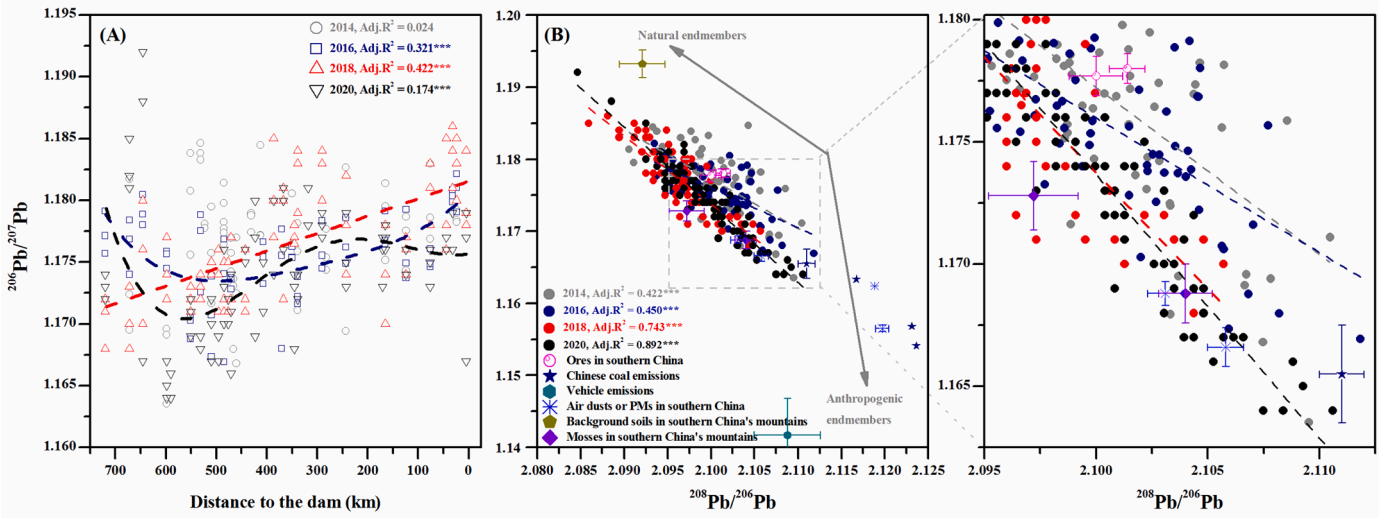

Fig. 6. Spatial and temporal variations of $^{206}Pb/^{207}Pb$ in the sediments of the WLF zone during 2014–2020 (A) and the diagrams of $^{206}Pb/^{207}Pb$ versus $^{208}Pb/^{206}Pb$ in the sediments with other reports from various potential Pb source materials (B). The fitting curves (except 2014) show the significant spatial trend of $^{206}Pb/^{207}Pb$ towards the dam ($p < 0.001$). The right sub-figure in Fig. 6B further highlights the Pb isotopic ratios in the range of the anthropogenic signals, which features much more plots within the range of the lower $^{206}Pb/^{207}Pb$ and higher $^{208}Pb/^{206}Pb$ with time. The references of the Pb isotopic ratios in the ores, coal combustion, vehicle exhaust, air dusts or aerosols, background soils and mosses in southern China were from Bi et al. (2017) and Bing et al. (2019b, H.J. 2021, and the references therein). ***, $p < 0.001$.

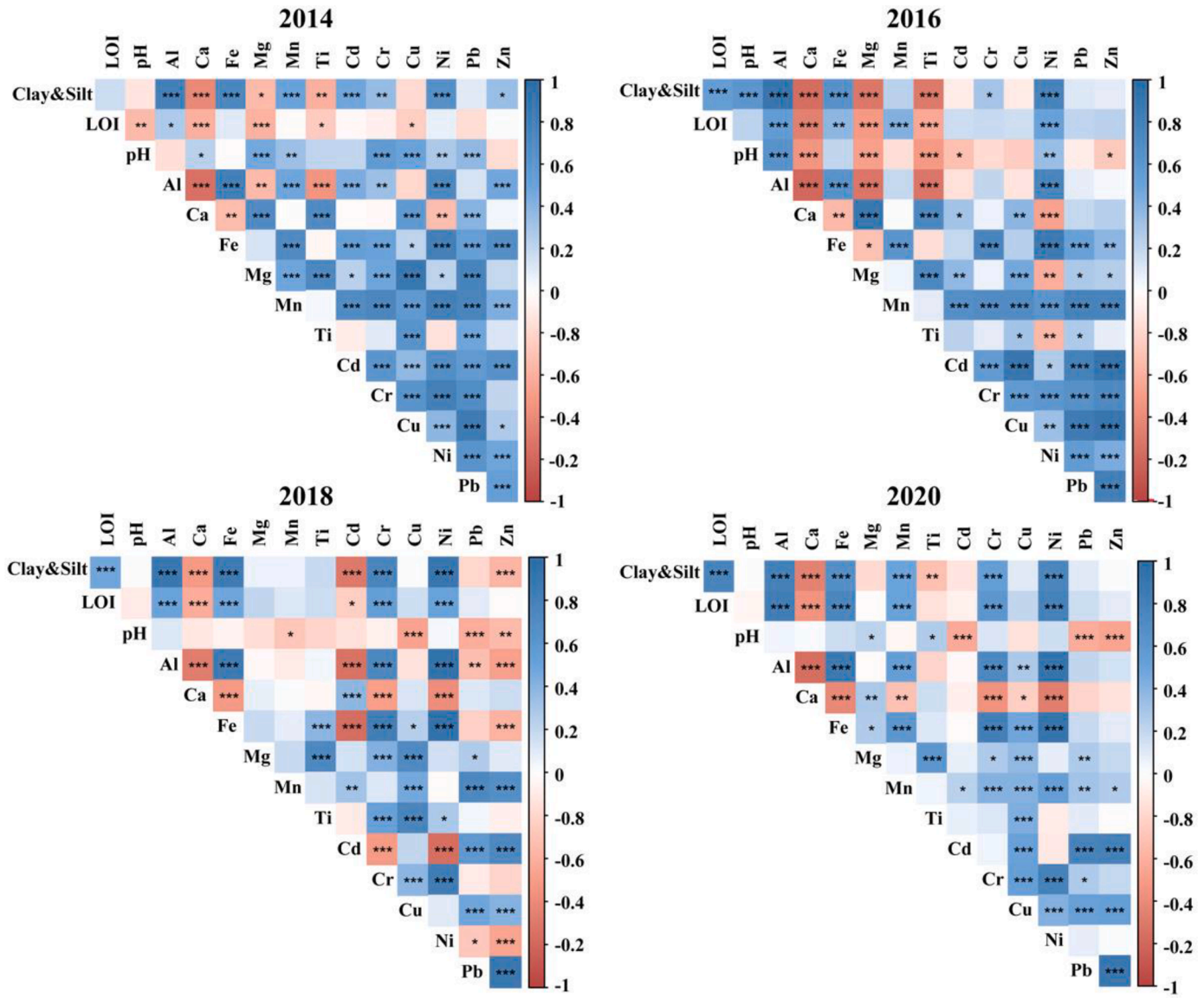

Fig. 7. Correlation of trace metals with each other and with sediment properties according to the Spearman correlation analysis.

metals also indicates that redox conditions and carbonates play an important role in the behavior of trace metals and affect their distribution in the sediments (Rinklebe et al., 2019; Shaheen et al., 2016).

Spatial information on regional human activities indirectly reflects anthropogenic effects on trace metal contamination in sediments. The higher concentrations and contamination levels of Cd, Pb, and Zn in the sediments were mainly centralized in the upper section of the TGR from 2016 to 2020 (Fig. 3), which corresponds to the main urban area of Chongqing City. Relatively, low ratios of $^{206}Pb/^{207}Pb$, which commonly represent anthropogenic signals in China, were also observed in this area (Fig. 6A). Chongqing City is one of the most developed cities and industrial centers where there are many medium-sized enterprises involved in electroplating, machinery manufacturing, mineral mining, smelting, etc., and coal is one of the main industrial fuel and energy sources in urban areas (Wang et al., 2006). Consequently, the discharges of industrial and municipal sewage from the main urban area were markedly higher than those from other areas in the TGR region (Figure S5a), which strongly supports the anthropogenic contribution of Cd, Pb, and Zn in the sediments. Moreover, we also sampled the sediments in the upper, outside the TGR (the background site at Zhutuo) from 2016 to 2020, and the results showed that the concentrations of all trace metals in the sediments were notably lower at the background site than in the WLF zone, despite a small temporal difference (Table S3). This indicates that the distant inputs of trace metals from the upper Yangtze River had a limited contribution to metal contamination in the sediments of the TGR relative to the main urban area. In addition, relatively high contamination levels of trace metals were observed in the middle section of the TGR during 2016–2020 and in areas near the dam in 2014 and 2020 (Fig. 5). Agricultural and animal husbandry industries may have caused trace metal accumulation in the sediments of the middle section, which features a relatively flat and wide area via runoff and/or seepage. However, the high values in the areas near the dam were possibly associated with the high geological background levels of the trace metals in the host rock (limestone), considering the fewer cities and less-developed industries (Bao et al., 2015; Zhao et al., 2020).

4.2. Regulation of sedimentary dynamics on the spatiotemporal distribution of trace metals

In this study, we observed that the concentrations and contamination of trace metals in the sediments increased markedly after the full impoundment stage of the TGR relative to the early stage, especially for

Cd, which reached its highest contamination in 2018 and then decreased in 2020 (Fig. 2, Table 2). As discussed above, the sediments from the upper Yangtze River commonly contain fewer trace metals and are regarded as a "clean" provenance, in that they limit the contribution of trace metals to the WLF zone of the TGR. Therefore, the decreased distant inputs of sediments and their bound trace metals from the upper Yangtze River further enlarges the role of anthropogenic contribution in the urban area in metal accumulation in the sediments. This was also supported by the negative or non-significant correlation of anthropogenic metals (e.g., Cd, Pb, and Zn) with Al and Fe in 2018 and 2020 (Fig. 7). However, sediment inputs from the upper Yangtze River may have two contrasting effects on the accumulation of anthropogenic metals in the sediments, as was observed for 2018 and 2020. According to the sediment discharge data from the monitoring stations, there was a marked increase in the fluxes of sediment discharge in both 2018 and 2020, and the fluxes were much higher in 2020 than in 2018 (Figure S6). Thus, we infer that the increased sediment fluxes along with the finer grain size in 2018 accelerated the adsorption and deposition of anthropogenic metals in the WLF zone, while the higher sediment inputs and a slightly coarser grain size in 2020 relative to those in 2018 diluted the concentrations of these metals. This is also supported by the non-significant difference in Pb concentrations between 2018 and 2020, but the significantly lower $^{206}Pb/^{207}Pb$ ratios in 2020 relative to those in 2018 (Fig. 2, Table S2).

Spatially, three distribution patterns of anthropogenic metals (Cd, Pb, and Zn) were observed in the sediments of the WLF zone over the four years (Fig. 3). Although human activities in the urban area of the TGR have become the major driver of trace metal accumulation in the sediments, the variations in the particle composition of sediments are considered to drive the trace metal distribution in the WLF zone. This is because fine-grained sediments have a relatively large specific surface area (Beckingham et al., 2016), and they can adsorb and transport trace metals at further distances. Our previous study found that with a decrease in the grain sizes, the fine particles in the sediments, which consisted of scattered coatings in a squama shape with more ridges, channels, and pores, tended to be more complex in terms of surface morphology and structure (Wang et al., 2020). In the present study, we also observed that the proportion of fine particles in sediments increased significantly with increasing impoundment time. Moreover, the contents of fine particles, Al, and Fe (relatively high element composition in mineral) displayed a clear spatial variation with distance to the dam from 2014 to 2020 (Fig. 1). Namely, their contents gradually increased from upstream to downstream of the TGR in 2014, while relatively higher contents appeared further from the dam after 2014, especially in 2018, when higher values were observed in the middle and upper sections. Considering that the sediments entering the TGR decreased sharply, but the runoff did not vary significantly in 2014 (Figure S6), the sampled sediments in 2014 probably recorded the signal before 2014 with the higher contents of relatively coarse particles when compared with other years. As a result, the fine particles were transported long distances to the near-dam areas, resulting in the high deposition of bound trace metals. With the continuous sediment interception by the cascade reservoirs and the water and soil conservation measures implemented in the upper Yangtze River and the increasing fine particles under the decrease in flow velocity in the middle and upper sections, the trace metals emitted by local human activities can be adsorbed by fine-grained sediments and promptly deposited in the WLF zone.

Overall, anthropogenic emissions in the main urban area of the TGR have become a main driver of the spatial distribution of trace metals in the sediments of the WLF zone, while sediment composition regulates the transportation and deposition of anthropogenic metals. Recently, increasing research with model prediction has revealed a decreasing trend of sediment inputs into the TGR (Tian et al., 2021), which may stress the human disturbance on trace metal accumulation in sediments. However, two issues must be noted when evaluating the sedimentary dynamics of trace metal distribution in the sediments of the WLF zone. First, fluvial sediments can store substantial trace metals, which may introduce a lag period into the transport and deposition of trace metals. Thus, legacy metal contamination in the sediments may have affected their spatial distribution. It should be noted that we have considered this issue by collecting surface sediments every two years. Second, extreme climate events and their induced flooding in the upper Yangtze River have evidently increased in recent years (Li et al., 2021), therefore also significantly affecting the runoff and sediment discharges in the TGR region. For example, relative to the periods before 2014, the annual precipitation in the TGR area generally increased according to the local weather stations (Figure S7 A and B). More importantly, extreme precipitation events increased markedly in the summer, although the annual precipitation did not change significantly or even decreased (Figure S7 C and D). In particular, rainfall in 2020 caused five flooding events with discharges over 50,000 m^3/s in the Yangtze River basin (Xia and Chen, 2021), and the station of Cuntan in the upper Yangtze River recorded the second highest water level since 1892 (Bulletin of the Sediments in the Yangtze River, http://www.cjw.gov.cn/zwzc/bmgb/2020 gb/). These extreme events have resulted in evident variations in runoff and sediment discharges in the TGR (Figure S6), which is a potential driver of the changes in the deposition and distribution of anthropogenic metals. Therefore, in addition to long-term monitoring of sediment inputs from the upper Yangtze River, the annual sediment dynamics regulated by extreme climate must be considered to prevent trace metal contamination in the aquatic environment.

4.3. *Attenuation of trace metal contamination in water driven by sedimentary dynamics*

The TGR operation features an anti-seasonal water-level regulation, with the lowest in the wet seasons and the highest in the dry seasons, which may cause trace metals in the sediments to be released to the overlying water via diffusion, dissolution, and exchange, especially at high water levels and relatively anaerobic conditions. The positive relationship between anthropogenic metals in the water and their labile fractions in the sediments confirms the direct contribution of trace metal release from sediments to the overlying water (Figure S3). However, according to the trace metal concentrations in the water, water quality is generally at an acceptable level for aquatic organisms in the TGR (Table 1). When compared with other reports using the health risk index (Zhao et al., 2017, 2020), there was no potential health risk of the studied trace metals for the local population. Meanwhile, we also observed a decreasing trend of the trace metal concentrations since dam construction, and the decrease was much more significant after the full impoundment stage (Table 1), which indicates that dam construction may be unexpectedly conducive to improving the water quality away from trace metal contamination. In contrast, we found the opposite case of trace metal accumulation in the sediments after dam construction (Fig. 2). This suggests that the decrease in trace metals in the water may be closely associated with the sedimentary dynamics under the current flow regulation of the TGR, which has altered the hydrological conditions and sediment deposition (Deng et al., 2016; Zhu et al., 2019), and the migration and accumulation of trace metals in the aquatic environment. After the full impoundment operation of the TGR, the flow velocity of the water decreased notably (Tang et al., 2016; Xiang et al., 2021), which increased the retention time of the sediments in the water and the sediment sorting and deposition. The recent study found that the suspended sediment concentration has declined by an order magnitude (from ~1.0 to 0.1 kg/m^3) in the heavily dammed Changjiang fluvial system in recent three decades (Sun et al., 2021). In this study, the increased content of fine-grained sediments from 2014 to 2020 also supports the increased deposition of fine particles in the TGR (Fig. 1). Considering the high adsorption capacity of fine particles for the elements, the decreasing concentrations of trace metals in the water are mainly attributed to the elevated water retention time and sediment

adsorption of the metals.

Although the spatial distribution of trace metals was similar in the water and sediments, the concentrations of individual metals were not significantly correlated between the water and the sediments, especially for anthropogenic metals (except Zn). On the one hand, the higher concentrations of trace metals such as Cd, Pb, and Zn in the water of the upper TGR further confirm the complex effects of anthropogenic emissions on their accumulation in the sediments. On the other hand, dynamic variations in the fluxes and particle composition of sediments may modulate the deposition of fine particle-adsorbed metals. Specifically, the content of fine-grained sediments in the middle and upper sections of the TGR increased from 2014 to 2020 (Fig. 1). The trace metals emitted by local human activities can be adsorbed in these fine-grained sediments and dynamically deposited in the WLF zone, especially in the high water-level season with decreased flow velocity and subsequent backflow (Bao et al., 2015), which is a probable reason for the non-significant relationship of each metal between the water and the sediments. Therefore, the sedimentary dynamics in the TGR have great potential for regulating trace metal contamination in water. Meanwhile, our results indicate that under the effects of the cascade dams constructed in the upper Yangtze River, the decrease in the sediment fluxes (mainly the decreased sediments with large grain sizes) and the increase in the fine sediment content contributed to the good water quality in the TGR.

5. Conclusions

In this study, we found a significant decrease in trace metal concentrations in the water of the TGR mainstream, especially since the dam operation, whereas the concentrations and contamination of anthropogenic metals (e.g., Cd, Pb, Zn, and Cu) in the sediments of the WLF zone increased notably. As expected, spatiotemporal variations in the contamination of these metals highlighted the importance of human activities in the urban area of the TGR. Moreover, the dynamic variations in the fluxes and composition of sediments under periodic and anti-seasonal flow regulation, as well as extreme climate, modulated the distribution patterns of trace metals in the sediments. In contrast to our previously thought, the higher anthropogenic contribution to trace metals relative to natural inputs did not negatively affect water quality, which may be closely related to the fine sediment composition with increasing impoundment time. Our results suggest that large dam construction in riverine systems, such as the TGR, probably prevents trace metal contamination from the water environment by regulating the fluxes and composition of sediments. However, the adsorption and release capacity of sediments for the trace metals over the long term still needs to be considered under in situ periodic water-level fluctuations in the future. Our results can serve as a foundation for future environmental impact assessments resulting from dam-induced river fragmentation and hydrological alterations, as well as for advanced management strategies to mitigate trace metal contamination in large reservoirs.

Declaration of Competing Interest

The authors declare that they do not have any competing interests that could have appeared to influence the work reported in this paper.

Acknowledgements

This work was supported by the CAS “Light of West China” Program, the Youth Innovation Promotion Association of CAS (2019313 and 2017424), and the Special Talent Project of Sichuan Province. The authors thank Zhongxian Soil and Water Loss and Non-point Source Pollution Monitoring Station of Three Gorge Reservoir, CAS, for the support of the filed work, and thank Dr. Jun Zhou, Dr. Hongyang Sun, Dr. Jipeng Wang, Dr. Xiaoxiao Wang, Ms. Zhongxiang Xiang and Ms. Zhilin Zhong for the field sampling.

Supplementary materials

Supplementary material associated with this article can be found, in the online version, at doi:10.1016/j.watres.2022.118419.

References

Baborowski, M., Büttner, O., Morgenstern, P., Jancke, T., Westrich, B., 2012. Spatial variability of metal pollution in groyne fields of the Middle Elbe—Implications for sediment monitoring. Environ. Pollut. 167, 115–123.
Bao, Y.H., Gao, P., He, X.B., 2015. The water-level fluctuation zone of Three Gorges Reservoir—a unique geomorphological unit. Earth-Sci. Rev. 150, 14–24.
Beckingham, L.E., Mitnick, E.H., Steefel, C.I., Zhang, S., Voltolini, M., Swift, A.M., et al., 2016. Evaluation of mineral reactive surface area estimates for prediction of reactivity of a multi-mineral sediment. Geochim. Cosmochim. Ac. 188, 310–329.
Bi, X.Y., Li, Z.G., Wang, S.X., Zhang, L., Xu, R., Liu, J.L., et al., 2017. Lead isotopic compositions of selected coals, Pb/Zn ores and fuels in China and the application for source tracing. Environ. Sci. Technol. 51, 13502–13508.
Bing, H.J., Wu, Y.H., Zhou, J., Ming, L.L., Sun, S.Q., Li, X.D., 2014. Atmospheric deposition of lead in remote high mountain of eastern Tibetan Plateau. China. Atmos. Environ. 99, 425–435.
Bing, H.J., Zhou, J., Wu, Y.H., Wang, X.X., Sun, H.Y., Li, R., 2016. Current state, sources, and potential risk of heavy metals in sediments of Three Gorges Reservoir. China. Environ. Pollut. 214, 485–496.
Bing, H.J., Wu, Y.H., Zhou, J., Sun, H.Y., Wang, X.X., Zhu, H., 2019a. Spatial variation of heavy metal contamination in the riparian sediments after two-year flow regulation in the Three Gorges Reservoir. China. Sci. Total Environ. 649, 1004–1016.
Bing, H.J., Wu, Y.H., Li, J., Xiang, Z.X., Luo, X.S., Zhou, J., et al., 2019b. Biomonitoring trace element contamination impacted by atmospheric deposition in China’s remote mountains. Atmos. Res. 224, 30–41.
Bing, H.J., Qiu, S.J., Tian, X., Li, J., Zhu, H., Wu, Y.H., Zhang, G., 2021. Trace metal contamination in soils from mountain regions across China: spatial distribution, sources and potential drivers. Soil Ecol. Lett. 3, 189–206.
Chen, J.M., Tan, M.G., Li, Y.L., Zhang, Y.M., Lu, W.W., Tong, Y.P., et al., 2005. A lead isotope record of Shanghai atmospheric lead emissions in total suspended particles during the period of phasing out of leaded gasoline. Atmos. Environ. 39, 1245–1253.
Chen, H., Teng, Y., Lu, S., Wang, Y., Wang, J., 2015. Contamination features and health risk of soil heavy metals in China. Sci. Total Environ. 512 (513), 143–153.
Cheng, H.F., Hu, Y.N., 2010. Lead (Pb) isotopic fingerprinting and its applications in lead pollution studies in China: a review. Environ. Pollut. 158, 1134–1146.
Chen, P., Deng, J.Y., Tan, G.M., Lu, J.Y., Jin, Z.W., Zhou, Y.J., et al., 2021. Prediction research on sedimentation balance of Three Gorges Reservoir under new conditions of water and sediment. Sci. Rep. 11, 19005.
Dai, Z., Liu, J.T., Wei, W., Chen, J., 2014. Detection of the Three Gorges Dam influence on the Changjiang (Yangtze River) submerged delta. Sci. Rep. 4, 1–7.
Deng, K., Yang, S., Lian, E., Li, C., Yang, C., Wei, H., 2016. Three Gorges Dam alters the Changjiang (Yangtze) river water cycle in the dry season: evidence from H-O isotopes. Sci. Total Environ. 562, 89–97.
Du Laing, G., Rinklebe, J., Vandecasteele, B., Meers, E., Tack, F.M.G., 2009. Trace metal behaviour in estuarine and riverine floodplain soils and sediments: a review. Sci. Total Environ. 407, 3972–3985.
Feng, L., Hu, C., Chen, X., Song, Q., 2014. Influence of the Three Gorges Dam on total suspended matters in the Yangtze Estuary and its adjacent coastal waters: observations from MODIS. Remote Sens. Environ. 140, 779–788.
Fu, B.J., Wu, B.F., Lu, Y.H., Xu, Z.H., Cao, J.H., Niu, D., et al., 2010. Three Gorges project: efforts and challenges for the environment. Prog. Phys. Geog. 34, 741–754.
Gao, B., Zhou, H.D., Yu, Y., Wang, Y.C., 2015. Occurrence, distribution, and Risk Assessment of the Metals in Sediments and Fish from the Largest Reservoir in China. RSC Adv, pp. 60322–60329.
Gao, Q., Li, Y., Cheng, Q.Y., Yu, M.X., Hu, B., Wang, Z.G., Yu, Z.Q., 2016. Analysis and assessment of the nutrients, biochemical indexes and heavy metals in the Three Gorges Reservoir, China, from 2008 to 2013. Water Res 92, 262–274.
Gao, L., Gao, B., Xu, D.Y., Peng, W.Q., Lu, J., 2019. Multiple assessments of trace metals in sediments and their response to the water level fluctuation in the Three Gorges Reservoir. China. Sci. Total Environ. 648, 197–205.
Grill, G., Lehner, B., Lumsdon, A.E., MacDonald, G.K., Zarfl, C., Reidy Liermann, C., 2015. An index-based framework for assessing patterns and trends in river fragmentation and flow regulation by global dams at multiple scales. Environ. Res. Lett. 10, 015001.
Grill, G., Lehner, B., Thieme, M., Geenen, B., Tickner, D., Antonelli, F., et al., 2019. Mapping the world’s free-flowing rivers. Nature 569, 215–221.
He, D., Wang, K., Pang, Y., He, C., Li, P.H., Li, Y.Y., et al., 2020. Hydrological management constraints on the chemistry of dissolved organic matter in the Three Gorges Reservoir. Water Res 187, 116413.
Huang, J.C., Zhang, Y.J., Bing, H.J., Peng, J., Dong, F.F., Gao, J.F., Arhonditsis, G.B., 2021. Characterizing the river water quality in China: recent progress and on-going challenges. Water Res 201, 117309.
Latrubesse, E.M., Arima, E.Y., Dunne, T., Park, E., Baker, V.R., d’Horta, F.M., et al., 2017. Damming the rivers of the Amazon basin. Nature 546, 363–369.
Li, X., Zhang, K., Gu, P.R., Feng, H.T., Yin, Y.F., Chen, W., Cheng, B.C., 2021. Changes in precipitation extremes in the Yangtze River Basin during 1960-2019 and the association with global warming, ENSO, and local effects. Sci. Total Environ. 760, 144244.

Lin, L., Li, C., Yang, W.J., Zhao, L.Y., Liu, M., Li, Q.Y., Crittenden, J.C., 2020. Spatial variations and periodic changes in heavy metals in surface water and sediments of the Three Gorges Reservoir. China. Chemosphere 240, 124837.
Loska, K., Wiechuła, D., Korus, I., 2004. Metal contamination of farming soils affected by industry. Environ. Int. 30, 159–165.
Luo, X.S., Yu, S., Zhu, Y.G., Li, X.D., 2012. Trace metal contamination in urban soils of China. Sci. Total Environ. 421 (422), 17–30.
Maavara, T., Chen, Q.W., Van Meter, K., Brown, L.E., Zhang, J.Y., Ni, J.R., Zarfl, C., 2020. River dam impacts on biogeochemical cycling. Nat. Rev. Earth Environ. 1, 103–116.
MacDonald, D., Ingersoll, C., Berger, T., 2000. Development and evaluation of consensus-based sediment quality guidelines for freshwater ecosystems. Arch. Environ. Contam. Toxicol. 39, 20–31.
Muller, G., 1969. Index of geoaccumulation in sediments of the Rhine River. GeoJournal 2, 108–118.
Nilsson, C., Reidy, C.A., Dynesius, M., Carman, R., 2005. Fragmentation and flow regulation of the world's large river systems. Science 308, 405–408.
Rauret, G., Lopez-Sanchez, J., Sahuquillo, A., Rubio, R., Davidson, C., Ure, A., Quevauviller, P., 1999. Improvement of the BCR three step sequential extraction procedure prior to the certification of new sediment and soil reference materials. J. Environ. Monit. 1, 57–61.
Ren, J.Q., Zhao, M.D., Zhang, W., Xu, Q.X., Yuan, J., Dong, B.J., 2020. Impact of the construction of cascade reservoirs on suspended sediment peak transport variation during flood events in the Three Gorges Reservoir. Catena 188, 104409.
Ren, S., Zhang, B.W., Wang, W.J., Yuan, Y., Guo, C., 2021. Sedimentation and its response to management strategies of the Three Gorges Reservoir, Yangtze River, China. Catena 199, 105096.
Rinklebe, J., Antoniadis, V., Shaheen, S.M., Rosche, O., Altermann, M., 2019. Health risk assessment of potentially toxic elements in soils along the central Elbe River. Germany. Environ. It. 126, 76–88.
Shaheen, S.M., Rinklebe, J., Frohne, T., White, J.R., DeLaune, R.D., 2016. Redox effects on release kinetics of arsenic, cadmium, cobalt, and vanadium in Wax Lake deltaic freshwater marsh soils. Chemosphere 150, 740–748.
Singh, K.P., Mohan, D., Singh, V.K., Malik, A., 2005. Studies on distribution and fractionation of heavy metals in Gomati River sediments—A tributary of the Ganges. India. J. Hydrol. 312, 14–27.
Sun, J., Zhang, F.Y., Zhang, X.F., Lin, B.L., Yang, Z.S., Yuan, B., Falconer, R.A., 2021. Severely declining suspended sediment concentration in the heavily dammed Changjiang fluvial system. Water Resour. Res. 57 doi.org/10.1029/2021WR030370.
Tang, Q., Bao, Y.H., He, X.B., Fu, B.J., Collins, A.L., Zhang, X.B., 2016. Flow regulation manipulates contemporary seasonal sedimentary dynamics in the reservoir fluctuation zone of the Three Gorges Reservoir. China. Sci. Total Environ. 548 (549), 410–420.
Tang, Q., Fu, B.J., Collins, A.L., Wen, A.B., He, X.B., Bao, Y.H., 2018a. Developing a sustainable strategy to conserve reservoir marginal landscapes. Natl. Sci. Rev. 5, 10–14.
Tang, Q., Collins, A.L., Wen, A.B., He, X.B., Bao, Y.H., Yan, D.C., et al., 2018b. Particle size differentiation explains flow regulation controls on sediment sorting in the water-level fluctuation zone of the Three Gorges Reservoir. China. Sci. Total Environ. 633, 1114–1125.
Tian, Q., Xu, K.H., Dong, C.M., Yang, S.L., He, Y.J., Shi, B.W., 2021. Declining sediment discharge in the Yangtze River from 1956 to 2017: spatial and temporal changes and their causes. Water Resour. Res. 57 e2020WR028645.
Wang, D., He, L., Wei, S., Feng, X., 2006. Estimation of mercury emission from different sources to atmosphere in Chongqing. China. Sci. Total Environ. 366, 722–728.
Wang, S.A., Fu, B., Piao, S., Lü, Y., Ciais, P., Feng, X., Wang, Y., 2016. Reduced sediment transport in the Yellow River due to anthropogenic changes. Nat. Geosci. 9, 38–41.
Wang, X.X., Zhou, J., Wu, Y.H., Bol, R., Wu, Y., Sun, H.Y., Bing, H.J., 2020. Fine sediment particle microscopic characteristics, bioavailable phosphorus and environmental effects in the world largest reservoir. Environ. Pollut. 265, 114917.
Xenopoulos, M.A., Lodge, D.M., 2006. Going with the flow: using species-discharge relationships to forecast losses in fish biodiversity. Ecology 87, 1907–1914.
Xia, J., Chen, J., 2021. A new era of flood control strategies from the perspective of managing the 2020 Yangtze River flood. Sci. China Earth Sci. 64, 1–9.
Xiang, R., Wang, L.J., Li, H., Tian, Z.B., Zheng, B.H., 2021. Water quality variation in tributaries of the Three Gorges Reservoir from 2000 to 2015. Water Res 195, 116993.
Xu, X.B., Tan, Y., Yang, G.S., 2013. Environmental impact assessments of the Three Gorges Project in China: issues and interventions. Earth-Sci. Rev. 124, 115–125.
Xu, X.Q., Deng, G.Q., Hui, J.Y., Zhang, X.H., Qiu, C.Q., 1999. Heavy metal pollution in sediments from the Three Gorges Reservoir area. Acta Hydrobiologica Sinca 23, 1–10.
Yang, H., Xie, P., Ni, L.Y., Flower, R.J., 2012. Pollution in the Yangtze. Science 337, 410.
Yang, H.F., Yang, S.L., Xu, K.H., Milliman, J.D., Wang, H., Yang, Z., et al., 2018. Human impacts on sediment in the Yangtze River: a review and new perspectives. Glob. Planet. Chang. 162, 8–17.
Yang, S.L., Milliman, J.D., Li, P., Xu, K., 2011. 50,000 dams later: erosion of the Yangtze River and its delta. Glob. Planet. Chang. 75, 14–20.
Yang, S.L., Milliman, J.D., Xu, K.H., Deng, B., Zhang, X.Y., Luo, X.X., 2014. Downstream sedimentary and geomorphic impacts of the Three Gorges Dam on the Yangtze River. Earth-Sci. Rev. 138, 469–486.
Zarfl, C., Lumsdon, A.E., Berlekamp, J., Tydecks, L., Tockner, K., 2015. A global boom in hydropower dam construction. Aquat. Sci. 77, 161–170.
Zhang, C., Yu, Z.G., Zeng, G.M., Jiang, M., Yang, Z.Z., Cui, F., et al., 2014. Effects of sediment geochemical properties on heavy metal bioavailability. Environ. Int. 73, 270–281.
Zhao, L.Y., Gong, D.D., Zhao, W.H., Lin, L., Yang, W.J., Guo, W.J., et al., 2020. Spatial-temporal distribution characteristics and health risk assessment of heavy metals in surface water of the Three Gorges Reservoir. China. Sci. Total Environ. 704, 134833.
Zhao, X., Li, T.Y., Zhang, T.T., Luo, W.J., Li, J.Y., 2017. Distribution and health risk assessment of dissolved heavy metals in the Three Gorges Reservoir, China (section in the main urban area of Chongqing). Environ. Sci. Pollut. Res. 24, 2697–2710.
Zhou, Z.Q., Xie, S.P., Zhang, R.H., 2021. Historic Yangtze flooding of 2020 tied to extreme Indian Ocean conditions. P. Natl. Acad. Sci. USA 118, e2022255118.
Zhu, H., Bing, H.J., Wu, Y.H., Zhou, J., Sun, H.Y., Wang, J.P., Wang, X.X., 2019. The spatial and vertical distribution of heavy metal contamination in sediments of the Three Gorges Reservoir determined by anti-seasonal flow regulation. Sci. Total Environ. 664, 79–88.